Signal and crosstalk analysis using optical convolution of transmitted optical signals

Ikechi A. Ukaegbu, Anel Poluektova, Elochukwu Onyejegbu, Aresh Dadlani, Hyo-Hoon Park

Ikechi A. Ukaegbu, Anel Poluektova, Elochukwu Onyejegbu, Aresh Dadlani, Hyo-Hoon Park, "Signal and crosstalk analysis using optical convolution of transmitted optical signals," Proc. SPIE 10912, Physics and Simulation of Optoelectronic Devices XXVII, 1091219 (26 February 2019); doi: 10.1117/12.2505099

Event: SPIE OPTO, 2019, San Francisco, California, United States

Signal and Crosstalk Analysis Using Optical Convolution of Transmitted Optical Signals

Ikechi A. Ukaegbu [a], Anel Poluektova[a], Elochukwu Onyejegbu[a], Aresh Dadlani[a], Hyo-Hoon Park[b]
[a]Department of Electrical & Computer Engineering, Nazarbayev University
53 Kabanbay Batyr Av., 010000 Astana, Kazakhstan; [b]Department of Electrical Engineering, Korea Advance Institute of Science and Technology, 291 Daehak-ro Yuseong-gu, Daejeon, 34141, Korea

ABSTRACT

An optical system which consists of a transmitter array, a fiber array, and a receiver array, experience some signal loss and crosstalk as the signals travel from the transmitter to the receiver. Signal loss and crosstalk occur at the interface between the light source (Vertical Cavity Surface Emitting Laser, or the VCSEL) and the fiber array, and also at the interface between the fiber array and the detector (photodetector). In order to obtain the real-time analysis of the transmitted and crosstalk signals, optical convolution is employed in this work. Optical convolution of the radiated signals (from the VCSEL) and the fiber array is performed to determine the signal intensity at the receiver end and also the amount of crosstalk in the array system. Transmitted signal intensity and crosstalk are essential for defining signal integrity and reliability during the packaging of optoelectronic transmitter and receiver modules in an optical system. A theoretical analysis of transmitted and crosstalk signals is performed with various separation distances between the transmitter modules and the fiber array and with a zero separation distance between the fiber array and the photodetector. The analysis is also performed for a top-emitting VCSEL (for the planar transmitter module) and bottom-emitting VCSEL (for the multi-chip transmitter module). The optical convolution allows us to obtain the real-time and the actual transmitted and crosstalk signals at the receiver end of an optical array system. It also provides optical system performance analysis.

Keywords: Optical convolution, Transmitted signals, Crosstalk

1. INTRODUCTION

Optical interconnection technology is seen as a promising technology to meet the high bandwidth and high-speed requirements of the next generation computer systems. Optical interconnects exhibit several advantages over electrical interconnects such as low power consumption, high bandwidth, and low inter-channel crosstalk. In order to achieve larger throughput of high speed signals from one point to another in the computer systems, there is need for multi-channel optoelectronic and optical link systems. Some of such links might be between chips or boards. However, most of the optoelectronic and optical components used in optical interconnection technology require electrical interconnects for power and signal transmission. These electrical interconnects affect the overall performance and bandwidth of the optical link. As clock frequency increases, reaching the gigahertz/terahertz band and signal transmission rate reaching the gigabit/terabit range, signal integrity issues between parallel signal paths, such as crosstalk, become serious issues in multichannel/multi-conductor interconnects. Crosstalk is the phenomenon where energy is coupled from one signal path onto another in parallel multichannel links. Crosstalk could be electrical, when electromagnetic fields from links and structures surrounding them interact; optical, when optical power in one channel is coupled to an adjacent channel at the interconnect points along the optical link; or both electrical and optical.

As the demand for high speed and high data-rate optoelectronic chips and components increases, chip integration technology is experiencing a lot of improvements where new forms of interconnect and packaging techniques are being witnessed [1]. Such techniques include flip-chip bonding in multichip modules (MCM). Though wire-bonding technology is the most widely used technology for electrical interconnects between chips, flip-chip bonding technology is attracting a lot interest in optoelectronic interconnects [2] due to reduced interconnect length and reduction in electrical parasitics [3]. These packaging technologies are possible due to various structures of the optoelectronic interconnect components such as the light source in the optical link, namely, the VCSELs (Vertical Cavity Surface Emitting Lasers). In view of these structures, 4 VCSEL types have been utilized in an optical link for transmission and

Physics and Simulation of Optoelectronic Devices XXVII, edited by Bernd Witzigmann,
Marek Osiński, Yasuhiko Arakawa, Proc. of SPIE Vol. 10912, 1091219 · © 2019 SPIE
CCC code: 0277-786X/19/$18 · doi: 10.1117/12.2505099

crosstalk analysis. These structures include: top-emitting VCSEL and bottom-emitting VCSEL, where the short-wavelength (850nm) and long-wavelength (1310nm) of each type are all considered.

In this work, we consider an optical system which consists of a transmitter array, a fiber array, and a receiver array. As light signals travel from the transmitter to the receiver, some signal loss and crosstalk occur. Signal loss and crosstalk occur at the interface between the light source (Vertical Cavity Surface Emitting Laser, or the VCSEL) and the fiber array, and also at the interface between the fiber array and the detector (photodetector). Several works have been dedicated to the performance and total crosstalk analysis of optoelectronic links [4], [5]. However, much attention have not been paid to the optical crosstalk component of the total crosstalk. Also, it is important to obtain the real-time analysis of the transmitted and crosstalk signals. In order to achieve this, optical convolution of the transmitted signal is employed in this work. Optical convolution of the radiated signals (from the VCSEL) and the fiber array is performed to determine the signal intensity at the receiver end and also the amount of crosstalk in the array system. A theoretical analysis of transmitted and crosstalk signals is performed with various separation distances between the transmitter modules and the fiber array and with a zero separation distance between the fiber array and the photodetector. The analysis is also performed for a top-emitting VCSEL (for the short- and long- wavelength VCSEL of the planar transmitter module) and bottom-emitting VCSEL (for the short- and long- wavelength VCSEL of the multi-chip transmitter module).

2. THE OPTICAL LINK

The block diagram of an optoelectronic link is shown in Figure 1. It is made up of a transmitter, an optical source, optical link/medium, a photodetector, and a receiver. An optoelectronic transmitter is made up of the transmitter and the optical source while an optoelectronic receiver is made up of a photodetector and a receiver. At the transmitter side, the transmitter converts the input signal from the electrical source into a large current used modulate the optical source. The light output propagates through the optical link/medium, which is optical fiber, free space or waveguide. The optical signal from the optical link/medium is collected by the photodetector, which generates an electric current. The optical signal is converted into electrical signals by the optoelectronic transmitter and is amplified to the required signal level.

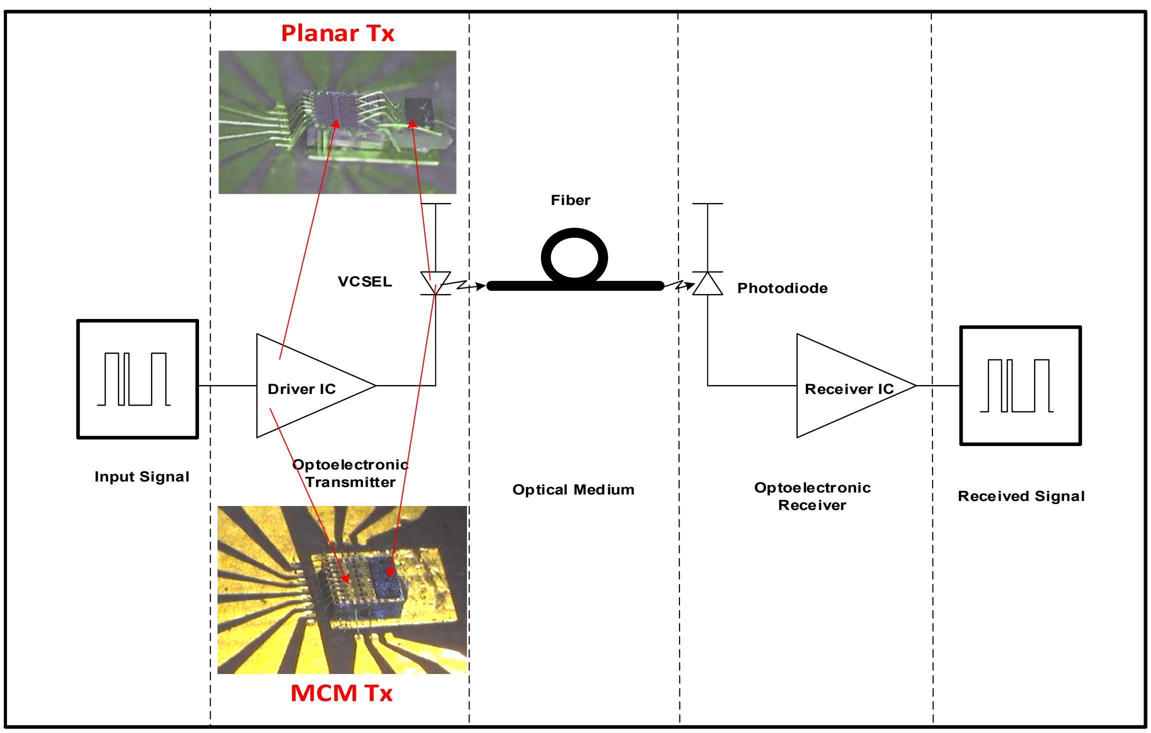

Figure 1. Block diagram of an optoelectronic link

In this work, we have designed two kinds of transmitter (Tx) module structures, namely, planar transmitter module and multichip transmitter modules. Each of these Tx modules were designed using four types of 1x4 VCSEL array chips, namely, short-wavelength (850nm) top-emitting VCSEL, long-wavelength (1310nm) top-emitting VCSEL, short-wavelength (850nm) bottom-emitting VCSEL, and long-wavelength (1310nm) bottom-emitting VCSEL. The characteristics of the VCSELs are shown in Table 1. In order to implement the transmitter modules, Teflon-based evaluation boards are used. The planar transmitter modules are prepared by attaching the driver IC and the 1x4 VCSEL array chips, separately on the evaluation board using conductive epoxy and wire-bonding technology. On the other hand, the MCM modules are prepared by flip-chip bonding the 1x4 VCSEL array chips to the driver IC. Gold stud bumps are used in the flip-chip bonding process. The bonded chips are then placed and bonded on the evaluation board using conductive epoxy and wire-bonding technology is used to make the necessary connect between the driver IC and the evaluation board. A photograph a planar (with top-emitting VCSEL) transmitter and MCM (with bottom-emitting VCSEL) are shown in Figure 1 as incepts.

Table 1: Electrical and optical characteristics of the short and long wavelength VCSELs

Parameter	VCSEL Type	Wavelength	Min	Typical	Max	Unit
Threshold current	Top	850 nm		1	2	mA
		1310 nm	1	1.4	2	
	Bottom	850 nm		1	2	
		1310 nm	1	1.7	2	
Output power	Top	850 nm		~1.0		mW
		1310 nm	0.5	~0.7		
	Bottom	850 nm		~1.0	2	
		1310 nm		~0.9	2	
Wavelength	Top	850 nm	840	850	860	nm
		1310 nm	1290	1310	1360	
	Bottom	850 nm	840	850	860	
		1310 nm	1290	1310	1360	
Beam divergence	Top	850 nm	15	20	25	deg
		1310 nm	7	9	11	
	Bottom	850 nm	15	20	25	
		1310 nm	7	9	11	
Aperture diameter	Top	850 nm		11		µm
		1310 nm		9		
	Bottom	850 nm		10		
		1310 nm		12		
Numerical aperture (NA)	Top (MM)	850 nm	0.13	0.2	0.26	
		1310 nm	0.13	0.2	0.25	
	Bottom (MM)	850 nm	0.13	0.2	0.26	
		1310 nm	0.13	0.2	0.25	

3. OPTICAL CONVOLUTION

Convolution is one of the most important and fundamental concepts in signal analysis and processing. If we know the impulse response of a system, then through convolution, it is possible to construct the output system of any arbitrary input signal. If we have an impulse, *f[n]* and impulse response, *h[n]*, then the output, *g[n]* is given as:

$$g[n] = f[n] * h[n] = \sum_{k=-\infty}^{\infty} f[k].h[n-k], \quad (1)$$

where * denotes convolution. In many signal processing problems, it is desirable to cross-correlate two signal. However, in this work, we consider a signal and a system. In order words, optical convolution in this work is defined as an operation between a signal and a system in which the input signal undergoes changes and the output is delivered. Our optical system is made up of an optoelectronic transmitter, a fiber system (propagation medium), and a receiver as shown in Figure 1 and described in section 2. Since the transmitter is made up of the driver IC and VCSEL chips, we will consider the VCSEL chips and their structures in this work. Thus, to perform optical convolution, we consider the radiated beams from the VCSELs and the nature of the surface from which the beams are radiated. The radiated beam and its nature is considered as the signal, while the fiber (propagation medium) is considered as the system.

4. SIGNAL ANAYISIS USING OPTICAL CONVOLUTION

4.1 Optical signal and the Gaussian beam

In this work, the optical signal from the VCSEL is considered as a Gaussian beam. The Gaussian beam, like most laser beams is collimated and almost monochromatic [6]. The distinguishing feature between Gaussian beams and other laser beams lies in the former's behavior along the path of propagation and in the transverse plane to this direction of propagation. In the plane transverse to the propagation direction, the intensity of the beam decreases in a typical Gaussian shape. Additionally, though the beam is collimated, it expands as it propagates [7]. To derive the mathematical representation of a Gaussian beam in 3-D, we start with a plane wave, the simplest type of 3-D waves [8]. A plane wave propagating long the z-direction is represented by the wave function:

$$\Psi(x,y,z,t) = Ae^{i(kz-\omega t)} \quad (2)$$

We then modify the constant amplitude of the plane wave in equation (2) to reflect a decrease in amplitude as the wave moves away from the source, along the direction of propagation (z-axis). Hence we have:

$$A = A(x,y) = e^{-(x^2+y^2)/\omega^2}, \quad (3)$$

where the beam width, $\omega_z = {}^{\omega_0}\sqrt{1+\frac{x^2}{z_R^2}}$, ω_0 is the beam waist, z_R denotes the Rayleigh range, λ is the wavelength of the beam. The beam width is also known as the beam spot. As stated earlier, Gaussian beam expands along the direction of propagation (z-axis in this case). Since the wave is expanding, the wavefront must be spherical [8]. This is because a wave always propagates in a direction perpendicular to its wavefront. The wavefront is defined as the surface that contains all points of the wave that carry the same phase. This spherical wavefront is not accounted fully by the plane-wave phase term e^{ikz}, so we must use a modified expression. The spatial part of a spherical wavefront has the form e^{ikr}, where $r = \sqrt{x^2+y^2+z^2}$. Suppose that we are examining the wave far from the origin but close to the z-axis such that $x \ll z$ and $y \ll z$. Then we can approximate r using the binomial approximation, to obtain

$$r = {}^{z}\sqrt{\frac{x^2+y^2}{z^2}+1} \cong z\left(1+\frac{x^2+y^2}{2z^2}\right) \quad (4)$$

Now with the adjustments to the plane wave equation in terms of amplitude, phase and wavefront, we can say that the equation of the Gaussian beam is approximated by:

$$\Psi(x,y,z,t) \approx e^{-(x^2+y^2)/\omega^2)} e^{i(kz-\omega t)} e^{ik(x^2+y^2)/2z)} \quad (5)$$

The first term contains the Gaussian profile, the second term has the unidirectional wave term, and the third term has the correction to the previous term that accounts for the curvature of the wavefront.

4.2 The optical fiber link and fiber transfer function

Optical fibers are usually categorized into single mode and multimode optical fibers. For single mode fibers, when the optical field is observed, only one spot is seen and it is single mode and the basic mode. However, for the multimode fiber, which has more than one mode, more than one spot is noticed in the optical field and the modes are of higher order than the basic mode. A step index fiber is made of a core and clad, where the single mode fiber has a smaller core when compared to a multimode fiber. In optical fibers, the V-number is usually used to describe the mode number of the optical fiber. When V < 2.405, the fiber can support only one mode and is said to be a single traverse mode fiber. But when V > 2.405, more than one mode is supported and the modes are represented with the mode number, M. The V-number is given by:

$$V = \frac{2\pi}{\lambda} a\sqrt{n_{Co}^2 - n_{Cl}^2} = \frac{2\pi}{\lambda} aNA, \qquad (6)$$

Where n_{Co} and n_{Cl} are the refractive indices of the fiber core and cladding, respectively; a denotes the core radius; and NA is the numerical aperture of the fiber. The relationship between the V-number and the mode number, M is given as:

$$M \approx \frac{4}{\pi^2} V^2 \qquad (7)$$

In this work, multimode fiber is used, where core/clad diameter is 100µm/110µm. Multimode fiber is used for easy coupling of light from the VCSEL to the fiber. Based on (6) and (7), M gives a large number of modes, which is of no consequence in our fiber system as it is only a few centimeters long. All the modes of the multimode fiber divert after they exit the fiber and overlap each other.

In the linear domain and for single mode fiber cables, the transfer function is given by the Fresnel sine and cosine integrals obtained using a recursive method called the Split-Step Fourier Transforms (SSFT) [9]. On the other hand, the Volterra Series Transfer Function (VSTF) or the Modified Volterra Series Transfer Function (MVSTF) is used to determine the transfer functions for both single mode and multimode fiber cables in the non-linear domain [9, 10]. These non-linear effects include the Self-Phase-Modulation Effects (SPM), Cross-Phase Modulation Effects (CPM), Stimulated Raman Scattering (SRS, Stimulated Brillouin Scattering (SBS) as well as the Four-Wave Mixing. It is important to note that non-linear effects in optical systems increase with increase in input power level as well as increases in the fiber length [9]. The Volterra Series Transfer Function (VSTF) itself is a mathematical tool than finds application in fields outside optics [11]. It is generally used to approximate the non-linear effects in a system.

Although the SSFT method incorporates the non-linear effects in the fiber cable in the time domain into the calculation of linear effects in the frequency domain, its recursive processes are considered a weakness, as it might introduce errors into the calculation [9]. We would however use both methods in our analysis of the effects on single mode optical fibers on light, then compare the results with empirical values to determine which of the methods gives the closest approximation experimental values. This is despite the fact that the input power/intensity of the input signal and the length of the fiber array used in this experiment suggests a linearity in the output characteristics fiber cable/array.

The generalized Non-Linear Schrödinger Equation (NLSE), shown below, is used to model all the known linear and non-linear effects of optical fibers.

$$\frac{\partial \mathrm{A}}{\partial \mathrm{z}} + \frac{\alpha_0}{2}\mathrm{A} + \beta_1 \frac{\partial \mathrm{A}}{\partial \mathrm{t}} + \mathrm{j}\frac{\beta_2}{2}\frac{\partial^2 \mathrm{A}}{\partial t^2} + \frac{\beta_3}{6}\frac{\partial^3 \mathrm{A}}{\partial t^3} = \mathrm{j}\gamma|\mathrm{A}|^2\mathrm{A} - a_1\frac{\partial(|\mathrm{A}|^2\mathrm{A})}{\partial \mathrm{t}} + a_2\frac{\partial \mathrm{A}}{\partial \mathrm{t}}|\mathrm{A}|^2 + a_3\frac{\partial|\mathrm{A}|^2}{\partial \mathrm{t}}\mathrm{A} + \mathrm{j}Q_R\mathrm{A} \times \int_{-\infty}^{\infty} s_r\,(\mathrm{t} - t_1)2|\mathrm{A}(t_1, \mathrm{z})|^2 \mathrm{d}t_1 \qquad (8)$$

Where A = A (t, z), A slowly varying complex envelop of the input pulse; α = Linear attenuation coefficient of the optical fiber; $\beta_1 = 1/v_g$ = Inverse of the optical carrier group velocity v_g; β_2= Second-order dispersion parameter usually called group velocity dispersion (GVD); β_3= Third-order dispersion parameter; $\gamma = \omega_0 / cA_{eff}n_2$; ω_0 = assigned as the central optical frequency of the carrier under consideration; A_{eff} is the effective cross section of the fiber and n_2 is the refractive index of the core section; $a_1 = a_0 / \omega_0$, a_2 and a_3 are the nonlinear coefficients of the single mode fiber; c is the speed of light; $Q_R = \omega_0 / cA_{eff}G_R$, is the Raman constant with G_R as the Raman gain coefficient factor; and $s_R(t)$ is the time-domain representation of the Raman gain spectrum $S_R(\omega)$. Equation (8) above cannot be solved analytically due to its non-linear nature. Numerical methods like the SSFT or the Runga-Kutta method are used to reach a final solution.

Frequency Domain Transfer Function is given by:

$$\mathrm{H}(\omega) = e^{(-j\beta_2\omega^2)} \tag{9}$$

And Time Domain Impulse Response is given by:

$$h(t) = \sqrt{\frac{1}{j4\pi\beta_2}}\ exp\ (\frac{jt^2}{4\beta_2}) \tag{10}$$

Based on [9], time domain step response in terms of Fresnel sine and cosine integrals is given as:

$$s(t) = \int_0^t \sqrt{\frac{1}{j4\pi\beta_2} exp\left(\frac{jt^2}{4\beta_2}\right) dt} = \sqrt{\frac{1}{j4\pi\beta_2}}\left[C\left(\sqrt{1/4\beta_2}\, t\right) + jS\left(\sqrt{1/4\beta_2}\, t\right)\right], \tag{11}$$

where $C(t) = \int_0^t cos\left(\frac{\pi}{2}\tau^2\right) d\tau$; $S(t) = \int_0^t sin\left(\frac{\pi}{2}\tau^2\right) d\tau$. As mentioned earlier, the weakness of most of the recursive methods in solving the NLSE is that they do not provide much useful information to help the characterization of non-linear effects. This is remedied by the VSTF which provides an elegant way of describing a system's nonlinearities. The Volterra series transfer function of a particular optical channel can be obtained in the frequency domain as a relationship between the input spectrum $X(\omega)$ and the output spectrum $Y(\omega)$ [9]:

$$Y(\omega) = \sum_{n-1}^{\infty} \int_{-\infty}^{\infty} \dots \int_{-\infty}^{\infty} H_n(\omega_1, \dots, \omega_{n-1}, \omega - \omega_1 - \dots - \omega_{n-1}) \times X(\omega_1) \dots X(\omega_{n-1}) X(\omega - \omega_1 - \dots - \omega_{n-1}) d\omega_1 \dots d\omega_{n-1} \tag{12}$$

where $H_n(\omega_1, \dots, \omega_n)$ is the nth-order frequency domain Volterra kernel including all signal frequencies of orders 1 to n. Since the fiber length used in this work is a few centimeters, we consider only the first term of the equation above, which is the solution for the first order transfer function. This is the linear transfer function of an optical fiber with the dispersion factors as defined previously. $A(\omega) = A(\omega,0)$, which is the amplitude envelope of the optical pulses at the input of the fiber. Thus the first order transfer function is given as [9]:

$$H_1(\omega, z) = e^{G_1(\omega)z} = e^{(-\frac{\alpha_0}{2} + j\beta_1\omega + \frac{j\beta_2}{2\omega^2} - \frac{j\beta_3}{6\omega^6})z} \tag{13}$$

Where $G_1(\omega) = -\frac{\alpha_0}{2} + j\beta_1\omega + \frac{j\beta_2}{2\omega^2} - \frac{j\beta_3}{6\omega^6}$; ω takes the values over the signal bandwidth and beyond in overlapping the signal spectrum of other optically modulated carriers, while $\omega_1 \dots \omega_3$ also take values over a similar range as that of ω.

4.3 Optical convolution of transmitted signals

In our optical system, optical convolution is performed between laser (VSCEL) beam and medium in which beam propagates (fiber system). Basd on (1) and substituting (5) and (13), the convolution equation for our system is given as:

$$g[n]=\frac{(2\sqrt{3}e^{-itw-\frac{x^2+y^2}{w^2}-\frac{u\alpha 0}{2}-\frac{1}{6}iuw(-6\beta 1+w(-3\beta 2+w\beta 3))}\left(\sqrt{\frac{1}{ikx^2+iky^2}}\sqrt{6ik+3\alpha 0+iw(-6\beta 1+w(-3\beta 2+w\beta 3))}\text{BesselK}[1,\frac{\sqrt{-6ik-3\alpha 0+iw(6\beta 1+w(3\beta 2-w\beta 3))}}{\sqrt{3}\sqrt{-\frac{1}{ikx^2+iky^2}}}\right)}{\left(\sqrt{-\frac{1}{i^2k^2(x^2+y^2)^2}}\sqrt{-(6ik+3\alpha 0+iw(-6\beta 1+w(-3\beta 2+w\beta 3)))^2}\right)}$$
$$+\frac{(2\sqrt{3}e^{-itw-\frac{x^2+y^2}{w^2}-\frac{u\alpha 0}{2}-\frac{1}{6}iuw(-6\beta 1+w(-3\beta 2+w\beta 3))}\left(\sqrt{-\frac{1}{ikx^2+iky^2}}\sqrt{-6ik-3\alpha 0+iw(6\beta 1+w(3\beta 2-w\beta 3))}\text{BesselK}[1,\frac{\sqrt{6ik+3\alpha 0+iw(-6\beta 1+w(-3\beta 2+w\beta 3))}}{\sqrt{3}\sqrt{\frac{1}{ikx^2+iky^2}}}]\right)}{\left(\sqrt{-\frac{1}{i^2k^2(x^2+y^2)^2}}\sqrt{-(6ik+3\alpha 0+iw(-6\beta 1+w(-3\beta 2+w\beta 3)))^2}\right)} \quad (14)$$

5. MEASUREMENT AND SIMULATION RESULTS

As reported in previous works [4], [5], [12], our optical interconnection scheme is based on fiber-embedded optical PCB, where the VCSEL based transmitter module is coupled onto a fiber input port. Based on the Gaussian beam equation of the VCSEL, the beam profile is plotted for various VCSEL types used in this work at different separation distances as shown in Table 1. Table 2 shows the bandwidth performance of the transmitted signals based on different transmitter module type at different separation distances between the VCSEL and the fiber. In Table 3, the optical crosstalk performance of the transmitted signals is show at various separation distances between the VCSEL and the fiber.

Table 1. Simulated Gaussian profile of the VCSEL beam at various separation distances from the fiber.

Separation distance	850 Bottom-emitting VCSEL Beam	1310 Bottom-emitting VCSEL Beam	1310 Top-emitting VCSEL Beam	850 Top-emitting VCSEL Beam
10 um	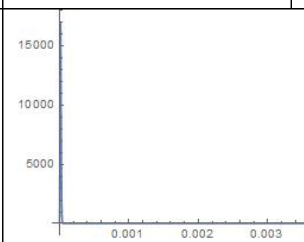	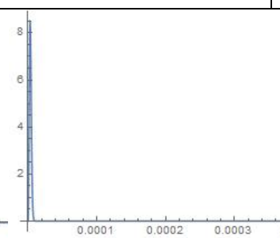	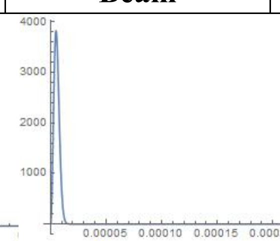	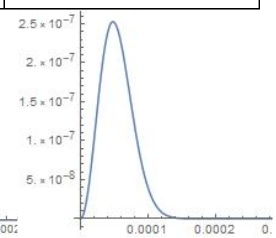
50 um	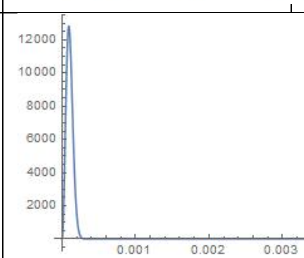	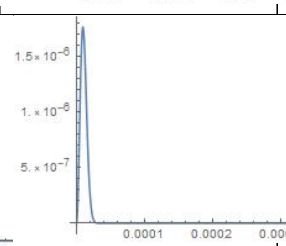	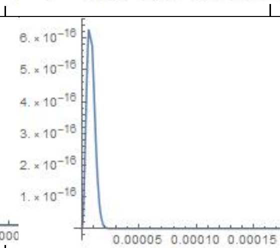	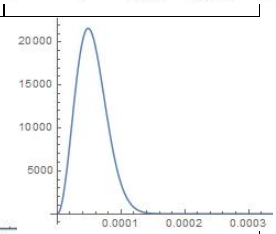
250 um	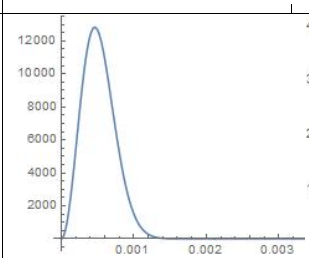	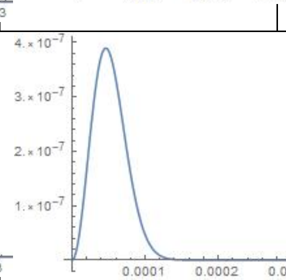	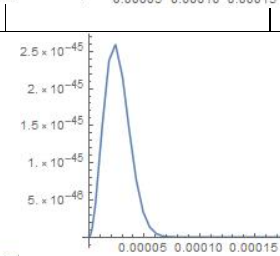	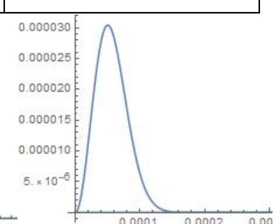

500 um

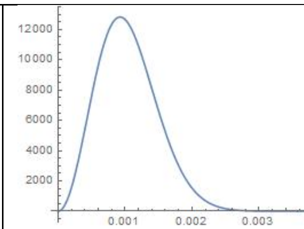

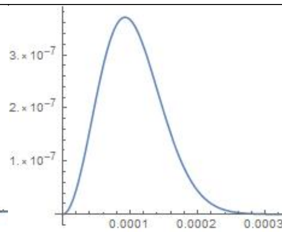

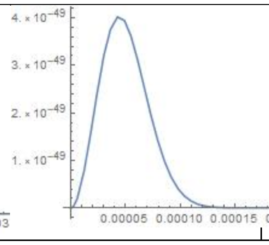

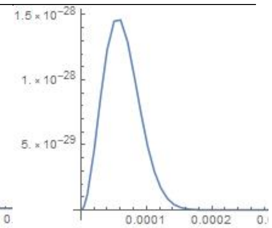

Table 2: Summary of measured bandwidth of transmitted signals at varying vertical distances between the VCSEL and the fiber link showing the bandwidth performance of each transmitter type

	Separation Distance, µm	**0**	**250**	**500**
850nm Top-emitting	-3-dB Bandwidth, GHz	4.57	4.27	3.96
1310nm Top-emitting	-3-dB Bandwidth, GHz	2.16	2.0	1.96
850nm Bottom-emitting	-3-dB Bandwidth, GHz	3.0	2.46	2.36
1310nm Bottom-emitting	-3-dB Bandwidth, GHz	2.46	2.16	2.0

Table 3: Summary of measured crosstalk at varying vertical distances between the VCSEL and the waveguide to show the effct of optical crosstalk contribution in the total crosstalk measurement

	Gap distance, µm	**0**	**250**	**500**
850nm Top-emitting	Crosstalk, @ < 1GHz dB	-53	-49.91	-37.9
	% optical crosstalk contribution		6.8%	28.5%
1310nm Top-emitting	Crosstalk, @ < 1GHz dB	-56.84	-55.0	-50.09
	% optical crosstalk contribution		3.2%	10.5%
850nm Bottom-emitting	Crosstalk, @ < 1GHz dB	-59.97	-56.27	-50.27
	% optical crosstalk contribution		6.2%	16.2%
1310nm Bottom-emitting	Crosstalk, @ < 1GHz dB	-62.56	-61.88	-58.57
	% optical crosstalk contribution		1.1%	6.4%

6. CONCLUSION

In this work, we are able to lay the groundwork for the application of optical convolution in optical systems for the main purpose of transmitted signal information and the optical crosstalk performance of the system. Optical convolution of the radiated signals (from the VCSEL) and the fiber array is performed to determine the signal intensity at the receiver end and also the amount of crosstalk in the array system. A convolution equation was obtained for the radiated signal through the fiber which could be applied for numerical signal analysis of signals at the receiver end. Measurement results were shown for the received signals where transmitted signal and crosstalk performance values are obtained.

REFERENCES

[1] A. Dickinson and M. M. Downs, "An optical multi-chip module," in Proc. of IEEE International Conference on Computer Design on VLSI in Computer and Processors (ICCD), pp. 490-493, 1991.

[2] K. Takahashi, T. Ikeuchi, T. Tsuda, and T. Chuzenji, "High speed multi-chip modules using flip chip mount technology for 10 Gbps transmission system," in *Proc. of Electronic Components and Technology (ECTC), 2001*, pp. 987-992, 2001

[3] D. Varoutas, A. Arapoyianni, and T. Sphicopoulos, "Modeling of electrical crosstalk in OIEC modules", *Fiber and integrated optics*, vol 24, pp91-111, 2005

[4] I. A. Ukaegbu, D.-W. Kim, M. H. Cho, T.-W. Lee, H.-H. Park, "Performance Analysis of Vertical and Horizontal Transmitter Array Modules Using Short and Long Wavelength VCSELs for Optical Interconnects," *IEEE Transactions on Components, Packaging and Manufacturing Technology*, vol. 3, no. 5, pp. 740-748, May, 2013

[5] I. A. Ukaegbu, J. Sangirov, M. H. Cho, T.-W. Lee, H.-H. Park, "Analytical Model for Crosstalk Analysis of Optoelectronic Transmitter Modules for Optical Interconnetcs," *Journal of Optical Engineering*, Vol. 50, no. 7, pp. 075401(1)-(8), July, 2011

[6] Galvez, E. J. (2009). *Gaussian Beams*

[7] G. P. Agrawal, "Spectrum-induced changes in diffraction of pulsed optical beams," *Opt. Commun.*, vol. 157, no. 1–6, pp. 52–56, 1998

[8] H. Kogelnik, "On the Propagation of Gaussian Beams of Light Through Lenslike Media Including those with a Loss or Gain Variation," *Appl. Opt.*, vol. 4, pp. 1562–1569, 1965

[9] L. N. Binh, "Linear and nonlinear transfer functions of single mode fiber for optical transmission systems," *J. Opt. Soc. Am. A*, vol. 26, no. 7, p. 1564, 2009.

[10] B. Xu and M. Brandt-Pearce, "Modified Volterra series transfer function method," *IEEE Photonics Technol. Lett.*, vol. 14, no. 1, pp. 47–49, 2002.

[11] M. Schetzen, The Volterra and Wiener Theories of Nonlinear Systems (Wiley, 1989)

[12] I. A. Ukaegbu, D.-W. Kim, M. H. Cho, T.-W. Lee, H.-H. Park, "2.5Gb/s/ch Long Wavelength Transmitter Modules for Chip-to-chip Optical PCB Applications," *IEEE Photonics Technol. Lett.*, vol. 23, no. 19, pp. 1403–1405, 2011.